Published in final edited form as:
Gene Ther. 2016 November ; 23(11): 767–774. doi:10.1038/gt.2016.54.

Single residue AAV capsid mutation improves transduction of photoreceptors in the *Abca4*$^{-/-}$ mouse and bipolar cells in the *rd1* mouse and human retina ex-vivo

Samantha R. De Silva[#1], **Peter Charbel Issa**[#1,2], **Mandeep S. Singh**[1], **Daniel M. Lipinski**[1], **Alona O. Barnea-Cramer**[1], **Nathan J. Walker**, **Alun R. Barnard**[1], **Mark W. Hankins**[1], and **Robert E. MacLaren**[1,3]

[1]Nuffield Laboratory of Ophthalmology, University of Oxford, NIHR Biomedical Research Centre, UK

[2]Department of Ophthalmology, University of Bonn, Bonn, Germany

[3]Moorfields Eye Hospital, NIHR Biomedical Research Centre, UK

[#] These authors contributed equally to this work.

Abstract

Gene therapy using adeno-associated viral vectors (AAV) for the treatment of retinal degenerations has shown safety and efficacy in clinical trials. However, very high levels of vector expression may be necessary for the treatment of conditions such as Stargardt disease where a dual vector approach is potentially needed, or in optogenetic strategies for end-stage degeneration in order to achieve maximal light sensitivity. In this study, we assessed two vectors with single capsid mutations, rAAV2/2(Y444F) and rAAV2/8(Y733F) in their ability to transduce retina in the *Abca4*$^{-/-}$ and *rd1* mouse models of retinal degeneration. We noted significantly increased photoreceptor transduction using rAAV2/8(Y733F) in the *Abca4*$^{-/-}$ mouse, in contrast to previous work where vectors tested in this model have shown low levels of photoreceptor transduction. Bipolar cell transduction was achieved following subretinal delivery of both vectors in the *rd1* mouse, and via intravitreal delivery of rAAV2/2(Y444F). The successful use of rAAV2/8(Y733F) to target bipolar cells was further validated on human tissue using an *ex-vivo* culture system of retinal explants. Capsid mutant AAV vectors transduce human retinal cells and may be particularly suited to treating retinal degenerations in which high levels of transgene expression are required.

Corresponding authors: Robert MacLaren, FRCOphth, DPhil, Nuffield Laboratory of Ophthalmology, University of Oxford, John Radcliffe Hospital, OX3 9DU, United Kingdom; Mark W Hankins PhD, Nuffield Laboratory of Ophthalmology, University of Oxford, John Radcliffe Hospital, OX3 9DU, United Kingdom, Tel: +44 1865 223380, enquiries@eye.ox.ac.uk.

Conflict of Interest

The authors have no conflict or relevant commercial interest to disclose. REM a Founder and Director of Nightstarx Ltd (Gibbs Building, 215 Euston Rd, London NW1 2BE) a choroideremia gene therapy company established by the University of Oxford and funded by the Wellcome Trust through Syncona Partners.

Europe PMC Funders Author Manuscripts

Introduction

Inherited retinal degenerations are in general a group of single gene diseases, which would potentially be amenable to gene therapy. Recent retinal gene therapy clinical trials using subretinally delivered serotype 2 adeno-associated viral vectors (AAV2) have shown safety and efficacy (1–4). Based on these studies together with data regarding safety of second eye administration (5) and long-term gene expression (6, 7), AAV2 remains the mainstay vector of choice for ocular use. However in order to optimize photoreceptor transduction, and possibly to administer vectors via intravitreal injection, efforts are ongoing to improve AAV transduction efficacy and alter cell tropism (8–10).

Early work concentrated on the use of natural variation in AAV biology and explored pseudotyped recombinant (r)AAV viral vectors, whereby vector expression cassettes containing the terminal repeats sequences of AAV2 were packaged into virions composed of capsid protein from other AAV serotypes (11). Using this principle, studies have shown improved primate photoreceptor transduction with the use of rAAV 2/8 over rAAV 2/2 (12).

More recently, mutation of the AAV capsid has been undertaken. Once internalized in the cell, AAV may be degraded by phosphorylation of exposed capsid tyrosine (Y) residues leading to ubiquitination and subsequent breakdown via the proteasome-mediated pathway. Phenylalanine (F) is less amenable to phosphorylation compared to tyrosine since it lacks a para-hydroxyl group. Tyrosine to phenylalanine mutation on the VP3 capsid protein of AAV2 has been demonstrated to increase transduction *in vitro* and *in vivo* (13), possibly by bypassing ubiquitin-mediated degradation of the virion shortly after intracellular entry (14).

Previous work examining retinal transduction by capsid mutant AAV examined multiple (two to seven) capsid mutations in rAAV2/2 (8). However minimizing the number of capsid mutations may be advantageous since these may alter antibody binding (15) and therefore the immune response. Further work compared single tyrosine mutations in self-complementary (sc) rAAV2/2, rAAV2/8 and rAAV2/9 (14), and also sc rAAV2/8(Y733F) in isolation (16, 17). AAV has a single stranded genome and therefore a rate-limiting step in AAV transduction is the generation of double stranded DNA. Self-complementary rAAV were designed to bypass this step since their single-stranded genome contains both forward and reverse copies of the transgene of interest with one wild type ITR and one mutated ITR. This enables the viral DNA to fold into a double stranded molecule after uncoating (18). These vectors have shown increased transduction efficacy in the eye (19), however, their effective coding capacity is limited since both forward and reverse copies of the transgene must be included (20).

The purpose of our study was to examine the effect on retinal transduction of a single tyrosine mutation in non self-complementary rAAV2/2(Y444F) (8, 13) and rAAV2/8(Y733F) (14) due to the larger coding capacity of these vectors compared to their self-complementary counterparts.

All vectors expressed green fluorescent protein (GFP) as a reporter protein. We examined cellular tropism of the mutant capsid rAAV vectors following subretinal delivery in wild type mice (WT, C57BL/6 strain) in comparison to the *Abca4*$^{-/-}$ mouse model. Mutations in

the gene coding for the ATP-binding cassette A4 (ABCA4) transmembrane transporter are among the commonest causes for inherited retinal dystrophies including Stargardt disease, with a key feature being accumulation of the bisretinoid N-retinylidene-N-retinylethanolamine (A2E) in the retinal pigment epithelium. *ABCA4* is a large transgene (6.7kb) and potential gene therapy for *ABCA4* mutations would require gene packaging in two AAV particles with the split gene recombining after infection of the cell (21, 22). For this to occur successfully, high transduction levels would be essential (23). We have previously shown that GFP expression following subretinal delivery of various AAV serotypes to *Abca4*$^{-/-}$ is significantly less than in WT mice, suggesting that accumulation of the lipofuscin fluorophore A2E in the outer retina inhibits AAV transduction in some way (24). We therefore assessed whether retinal transduction in this disease model would be more successful with capsid mutant AAV.

We also examined retinal transduction following subretinal and intravitreal delivery of capsid mutant AAV in *Pde6b*$^{rd1/rd1}$ mice. The *Pde6b* gene encodes the rod-specific cGMP phosphodiesterase β6 subunit (Pde6b^{rd1}) (25), and in this model there is rapid and severe rod photoreceptor degeneration followed by cone degeneration. This is therefore a model of end-stage retinitis pigmentosa where very few photoreceptors remain. A strategy for vision restoration in patients with end-stage RP is to use the technique of optogenetics, whereby a light sensitive protein is expressed in remaining retinal cells in the absence of photoreceptors. One such approach involves targeting bipolar cells to make them light sensitive (26), however, the tropism of unmodified rAAV vectors for bipolar cells is poor (24). Few previous studies have obtained adequate transduction to show functional improvement in this model, either using a self complementary AAV vector with a single capsid mutation (16), a synthetic AAV capsid (27) or one derived from a directed evolution approach (28). We therefore sought to assess whether capsid mutation of only a single residue in non self-complementary rAAV could improve retinal transduction in the *Pde6b*$^{rd1/rd1}$ model.

Recent studies have also demonstrated that retinal transduction using AAV may also differ between species, possibly due to differences in retinal morphology (29). In order to assess whether capsid mutant AAV would be suitable for use in future human clinical trials, we subsequently went on to test these vectors on human retinal tissue cultured *ex-vivo*.

Results

Retinal transduction in the *Abca4*$^{-/-}$ mouse following subretinal delivery of capsid mutant vectors

We have previously demonstrated that rAAV2/2 transduction is reduced in the *Abca4*$^{-/-}$ mouse model of retinal degeneration compared to WT mice (24). We therefore delivered single tyrosine mutant rAAV2/2(Y444F) and rAAV2/8(Y733F) by subretinal injection in both WT and *Abca4*$^{-/-}$ mice to assess transduction efficiency by these vectors.

***In vivo* measurement of fluorescence intensity—**Three weeks after subretinal injection, vector expression was assessed by measuring *in vivo* GFP fluorescence using *in vivo* confocal scanning laser ophthalmoscopy (cSLO) imaging. Ocular GFP fluorescence

was present in *Abca4*$^{-/-}$ and WT mice after injection of both of the test vectors, rAAV2/2(Y444F) and rAAV2/8(Y733F), and was confined to the area of subretinal vector injection (Figure 1a). By assessing mean pixel grey level as previously described (22, 28), significant differences in GFP fluorescence intensity were found between capsid mutant AAV types. Subretinal delivery of rAAV2/8 (Y733F) resulted in 4-fold higher expression in WT mice and 13-fold higher expression in *Abca4*$^{-/-}$ mice, than rAAV2/2(Y444F) (n=5-6 eyes per group, 2-way ANOVA $p<0.001$; Bonferroni post hoc test, both $p<0.001$, Figure 1b). No difference was seen in the expression of either vector between mouse strains.

Retinal cell tropism of capsid mutant AAV—*In vivo* fluorescence intensity measurements using cSLO images represent the combined fluorescence intensity of cells contained in multiple retinal layers. Therefore histological sections were examined to evaluate differences in transduction efficiency in specific retinal cell types. rAAV2/2 injected eyes were assessed as a reference to compare any difference in transduction pattern between vectors or mouse strain. RPE cell, photoreceptor, horizontal cell, bipolar cell, Müller cell and ganglion cell identity was determined on the basis of immunocytochemistry staining and cellular morphology.

Following subretinal vector delivery in both mouse strains, all vectors transduced RPE and photoreceptors to some degree (Figure 2a-f). Photoreceptor transduction however appeared to be most efficient using rAAV2/8(Y733F), with the highest levels of GFP expression. In the *Abca4*$^{-/-}$ mouse in particular, rAAV2/8(Y733F) was highly effective at transducing photoreceptors with levels of GFP expression being higher than both other vectors tested and also higher than in WT mice injected with the same vector, (n=5-6 eyes per group).

Fewer RPE cells were transduced by rAAV2/2(Y444F) in the *Abca4*$^{-/-}$ mouse compared to injection of the same vector in WT mice (Figure 2b&e, 3a). The tropism of rAAV2/2(Y444F) was markedly different to that of rAAV2/2 in both mouse strains, with more photoreceptor transduction, and less Müller cell and ganglion cell transduction using the capsid mutant vector (Figure 2).

Histological analysis of fluorescence intensity—In order to quantify transduction differences between the capsid mutant vectors, the quantification of GFP fluorescence was used as an indicator of transgene expression and therefore transduction efficiency. GFP fluorescence was determined by separately measuring the mean grey level in the RPE and outer nuclear layer in standardized histological preparations, which was then compared between rAAV serotypes and mouse strains (24).

There was a trend for RPE to be transduced more efficiently by rAAV2/8 (Y733F) than rAAV2/2(Y444F) ($p=0.09$), especially in the *Abca4*$^{-/-}$ mouse. However, neither viral type nor mouse strain had a statistically significant effect on RPE transduction (Figure 3a; 2 way ANOVA).

There was a significant difference in ONL transduction between rAAV serotypes ($p<0.01$) but not between mouse strains ($p=0.22$), and no significant interaction between the two factors ($p=0.17$) (Figure 3b; 2 way ANOVA). The most striking finding was significantly

increased ONL transduction in the *Abca4*$^{-/-}$ mouse using rAAV2/8(Y733F) compared to rAAV2/2(Y444F) ($p<0.05$, Bonferroni post hoc analysis). This difference in ONL transduction between vectors did not reach statistical significance in WT mice.

Tropism of capsid mutant vectors in the *Pde6b*$^{rd1/rd1}$ mouse

The *Pde6b*$^{rd1/rd1}$ mouse is a model of end-stage retinal degeneration, and targeting a light sensitive protein to bipolar cells in this model may restore visual function (26). However, these cells are difficult to transduce using rAAV, and we therefore aimed to assess if single capsid mutant rAAV vectors would be effective in transducing the retina in this model of degeneration.

Three weeks, after subretinal injection of rAAV2/2(Y444F) and rAAV2/8(Y733F) to *Pde6b*$^{rd1/rd1}$ mice with rAAV2/2 used for comparison, histological sections of the retina were examined to evaluate transduction and retinal cell tropism by these vectors (Figure 4a-c). All vectors tested were able to transduce RPE, horizontal cells and ganglion cells (supplementary figure 1). Similar to transduction in the WT retina, there was reduced Müller cell transduction with the use of rAAV2/2(Y444F) compared to rAAV2/2. Of note, both rAAV2/2(Y444F) and rAAV2/8(Y733F) capsid mutant vectors transduced bipolar cells effectively as shown by co-labeling for PKC alpha (Figure 4b i-iii, 4c i-iii). No bipolar cell transduction was observed with rAAV2/2.

The transduction efficiency of these vectors was also assessed following intravitreal delivery, to ascertain whether bipolar cells could also be transduced via this route. WT mice were used for comparison, to assess if any differences between vectors were consistent between strains. Following intravitreal vector delivery all vectors were able to transduce ganglion cells (Figure 5 a-f), although transduction with rAAV2/8(Y733F) was sparse in both WT and *Pde6b*$^{rd1/rd1}$ mice (Figure 5c,f). Examining morphology of transduced cells, there was some evidence of Müller cell and horizontal cell transduction by rAAV2/2 and rAAV2/2(Y444F). Significantly, rAAV2/2(Y444F) successfully transduced bipolar cells in both WT and *Pde6b*$^{rd1/rd1}$ mice as shown by co-labeling for PKC alpha (Figure 5b i-iii, 5e i-iii). As with subretinal delivery, no bipolar cell transduction was seen with intravitreal delivery of rAAV2/2.

Tropism of capsid mutant vectors in *ex vivo* human retinal culture

In order to assess whether the capsid mutant rAAV types tested in mice would be able to transduce human retina successfully, samples of human retina were obtained from patients undergoing complex surgery for retinal detachment in which a retinectomy procedure was performed as part of the operation. The retinal fragments obtained were maintained in an *ex vivo* culture system, as described previously (30, 31). Since successful human retinal transduction using rAAV2/2 has been demonstrated using this culture system (32), this was used for comparison.

Successful human retinal transduction was seen with all rAAV types tested (Figure 6). Using rAAV2/2 and rAAV2/2(Y444F), GFP was predominantly seen in the ONL, consistent with photoreceptor transduction (Figure 6 a,b). Sparse inner retinal transduction was also seen with rAAV2/2 (Y444F). Using rAAV2/8(Y733F), the transduction pattern appeared to be

different, with less GFP expression in the ONL compared to the other two vectors, but markedly more expression in the INL (Figure 6c). On the basis of cell morphology, Müller cell transduction is apparent with multiple characteristic branching cells that span the entire retina. Immunocytochemistry confirmed that rAAV2/8(Y733F) can transduce human bipolar cells effectively (Figure 6d).

Discussion

In this study we have assessed the retinal cell tropism and transduction efficiency of two recombinant AAV vectors with capsid mutations of a single tyrosine to phenylalanine residue, rAAV2/2(Y444F) and rAAV2/8(Y733F). The tropism of both vectors was evaluated *in vivo* in WT mice and two mouse models of retinal disease, *Abca4*$^{-/-}$ and the totally degenerate retina, since successful clinical strategies for these conditions would most likely require very high levels of AAV transduction. We also assessed our findings from both vectors with *ex-vivo* testing on the human retina. In both the WT and the *Abca4*$^{-/-}$ mouse, the rAAV2/8(Y733F) vector was highly effective at targeting photoreceptors when delivered subretinally. Our novel observation that transduction is highly efficient in the *Abca4*$^{-/-}$ mouse is important because vectors tested in this model in previous work have shown low levels of photoreceptor transduction (24). This raised the possibility that biochemical alterations induced by abnormal dimerization of vitamin A molecules might interfere with AAV transduction.

In these models, we provide data showing that a single capsid mutation significantly alters the tropism of rAAV2/2, enhancing photoreceptor transduction and reducing Müller cell tropism when delivered subretinally. In the *Pde6b*$^{rd1/rd1}$ model, the same AAV2 capsid mutation enabled bipolar cell transduction in the degenerate retina when delivered via both subretinal and intravitreal routes. We also show bipolar cell transduction in human retinal explants using rAAV2/8 (Y733F).

While the rAAV2/8(Y733F) vector showed increased transduction efficiency in the *Abca4*$^{-/-}$ mouse compared to WT, there was no such effect of the AAV2 capsid mutation. However, previous assessments using rAAV2/2, rAAV2/5, as well as two novel hybrid recombinant AAV serotypes showed lower transduction in *Abca4*$^{-/-}$ compared to WT mice,(24) whereas rAAV2/2(Y444F) showed similar efficiency in both strains. Thus, there might be enhanced photoreceptor transduction using both single residue AAV capsid mutant vectors in *Abca4*$^{-/-}$mice. This is likely to be mediated by altered ubiquitination and proteasome-mediated breakdown, since our *in vitro* studies demonstrated increased rAAV2/2 transduction in the presence of proteasome inhibitors, but no such effect is seen with rAAV2/2(Y444F) (supplementary figure 2), consistent with previous reports (13). The low transduction efficiency seen with some vectors in the *Abca4*$^{-/-}$ mouse may be caused by the disease process induced by this mutation, however strain background effects may also be a contributing factor since WT mice were C57BL/6 and *Abca4*$^{-/-}$were on a 129S background (these WT controls were chosen to due to differences in background autofluorescence between mouse strains (33)). It remains to be investigated to what extent the superior efficiency of rAAV2/8(Y733F) is explained by the mutated capsid or rather due to a more general improved receptor-mediated uptake of AAV8 virions compared to other serotypes.

We also demonstrate that rAAV2/2(Y444F) can transduce WT retina effectively, however tropism was altered by this single capsid mutation with greater photoreceptor transduction and reduced Müller cell transduction compared to rAAV2/2. It has previously been proposed that AAV capsid mutations may alter retinal penetration (8), however this is unlikely to explain the reduced Müller cell tropism since these span the entire width of the retina. Other work has also demonstrated that mutations of the AAV capsid may affect heparan sulfate proteoglycan binding capacity (34) and this could contribute to the altered Müller cell tropism seen.

Inducing light sensitivity in bipolar cells in the degenerate retina may be an important optogenetic strategy for restoring vision (26), and therefore identifying a vector that can successfully target bipolar cells is essential. rAAV2/2 vectors with quadruple and pentuple capsid mutations have been shown to transduce bipolar cells when delivered by both the subretinal and intravitreal route in WT mice (8). Our findings indicate a vector with a single capsid mutation, rAAV2/2(Y444F), can be used to transduce bipolar cells when delivered by both the subretinal and intravitreal route in the *Pde6b*$^{rd1/rd1}$ model of degeneration. Therefore for future clinical trials in optogenetic strategies, rAAV2/2(Y444F) could be administered intravitreally to transduce bipolar cells which might avoid the need for intraoperative retinal detachment in patients with advanced retinal degeneration. The ability to do so with a single capsid mutant rAAV2/2 vector may be advantageous as although capsid mutation increases infectivity, this may be at the expense of altering antibody binding (15) and therefore immune responses. Thus for clinical trial applications it may be prudent to limit capsid mutation as much as possible in order to limit deviation from the presumed optimally evolved AAV structure.

A previous study in the *rd10* mouse model of retinal degeneration identified bipolar cell transduction using a self complementary rAAV2/8(Y733F) with transgene expression driven by a bipolar cell-specific promoter (16). We also show that a single stranded rAAV2/8(Y733F) vector is able to target bipolar cells in another mouse model (*Pde6b*$^{rd1/rd1}$) and using a ubiquitous and different promoter to that which has been previously reported. Significantly, this vector was also successful at targeting bipolar cells in *ex-vivo* human retinal explants. Retinectomy tissue from patients that had chronic retinal detachment was used, which was placed in culture immediately after removal from the eye, making it more likely to be viable for transduction by AAV than post-mortem tissue used in previous studies (35). However there may have been a variation in the baseline severity and nature of pathologic retinal changes among the retinal samples thus obtained, as the duration of preoperative retinal detachment and amount of proliferative vitreoretinopathy (PVR) was different between tissue samples. Therefore, the human retinal transduction patterns reported here may be affected by these factors which may explain the limited photoreceptor transduction seen with AAV2/8(Y733F). The high level of Müller cell transduction seen in the human retinal explants when transduced with rAAV2/8(Y733F) may be related to the extensive glial cell proliferation is known to be a feature of retinal detachment. Nevertheless some glial cell activation is also likely to occur in end stage retinal degenerations and the observation of efficient AAV transduction in the degenerate human retina may therefore be relevant.

In summary, we report effective retinal transduction with two single-stranded capsid mutant vectors in WT mice and in two mouse models of human retinal disease in which high levels of AAV transduction would most likely be required. In addition, we demonstrate human bipolar cell transduction in an *ex-vivo* culture system using rAAV2/8(Y733F).

Methods

Viral vectors

rAAV2/2, rAAV2/2(Y444F) and rAAV2/8(Y733F) used in our study were designed by REM based on published observations from other groups (14, 16). Capsid mutant vectors were generated by site-directed mutagenesis of surface-exposed tyrosine residues on AAV capsid VP3 as previously described (13) and custom cloned by Genedetect (Auckland, New Zealand). All vectors expressed green fluorescent protein (GFP) under the control of the same CMV-enhanced chicken beta-actin (CAG) promoter and included an X-antigen deleted Woodchuck hepatitis virus posttranscriptional regulatory element (WPRE) and bovine growth hormone polyadenylation signal, similar to the sequences used in an ongoing choroideremia gene therapy clinical trial (4). Vectors were purified by iodixanol gradient centrifugation and titres were confirmed by PCR to the promoter region.

Mice

Wild type (WT) C57BL/6 mice were provided by the Biomedical Sciences division, University of Oxford. C3H/HeNHsd-*Pde6b*^{rd1} (herein referred to as *Pde6b*$^{rd1/rd1}$) mice were purchased from Harlan Laboratories (Hillcrest, UK). Founder *Abca4* knockout mice (129S4/SvJae-*Abca4*$^{tm1Ght/tm1Ght}$, herein referred to as *Abca4*$^{-/-}$) were generously provided by Gabriel Travis, David Geffen School of Medicine, University of California, Los Angeles, USA.(36) and bred locally at the University of Oxford.

Animals were housed under a 12 hour light (<100 lux) / dark cycle, with food and water available *ad libitum*. All procedures were performed under the approval of local and national ethical and legal authorities and in accordance with the Association for Research in Vision and Ophthalmology statements on the care and use of animals in ophthalmic research.

At the time of intraocular injection, mice were between 6 and 8 weeks old. For surgery and *in vivo* imaging procedures, animals were anesthetized by intraperitoneal injection of 1 mg/kg medetomidine (Dormitor 1 mg/mL, Pfizer, Sandwich, UK) and 60mg/kg ketamine (Ketaset 100mg/mL, Fort Dodge, Southampton, UK) and pupils fully dilated with tropicamide 1% eye drops (Bausch & Lomb, Kingston-Upon-Thames, UK) and, for the imaging procedure, phenylephrine 2.5% eye drops (Bausch & Lomb, Kingston-Upon-Thames, UK).

Intraocular injections

Intra-ocular injections were performed tangentially through the sclera with a 10mm 34-gauge needle (Hamilton AG, Bonaduz, Switzerland) mounted on a 5μl syringe (65 RN, Hamilton AG) under direct visual control using a surgical microscope (M620 Leica). A circular cover glass (Ø6mm, VWR International, Lutterworth, UK) was applied onto the

cornea with a carbomer coupling gel (Viscotears, Novartis, Frimley, UK) to ensure good visualization of the fundus. The eye position was controlled and stabilized by holding the superior or inferior rectus muscle with notched forceps. 1μl viral vector solution (1.0×10^{12} vg/mL) was injected into each eye, and complete subretinal or intravitreal delivery was confirmed by direct visualization. After injection, the needle was left in position for an additional 20-30 seconds and then withdrawn quickly to minimize reflux and to allow self-sealing of the scleral tunnel. Each animal received a different viral type in each eye, with different syringes and needles used for the different viruses. Between individual injections, the needle and syringe was flushed with sterile water. For WT (C57BL/6) mice and C3H/HeNHsd-*Pde6b*^{rd1} mice, 5 eyes were injected for each virus tested (the same virus was not tested in both eyes of a mouse). For ABCA4$^{-/-}$ mice 6 eyes were injected per virus tested.

Fundus imaging using a confocal scanning laser ophthalmoscope

Three weeks after intraocular injection, confocal scanning laser ophthalmoscope (cSLO; Spectralis HRA, Heidelberg Engineering, Heidelberg, Germany) imaging was performed under general anesthesia (as above) according to a modified protocol that has been described in detail previously.(37) In brief, the pupils were fully dilated and a custom-made mouse contact lens (Cantor-Nissel) placed on the cornea. The near-infrared (NIR) reflectance mode (820 nm laser) was used for camera alignment. For recordings from the outer or inner retina, the plane of highest NIR reflectivity or the plane of the nerve fibre layer was identified, respectively. After switching to the autofluorescence mode (excitation wavelength: 488 nm, emission collection 500-700 nm) and slight focus adjustments (due to the dioptric shift between the different wavelengths), images were recorded with a standardized detector sensitivity of 70 using the automated real time (ART) mode, without image normalization. All images were recorded in the high-resolution mode (1536×1536 pixels) using a 55 degree lens.

Tissue collection and processing

After the imaging procedure, mice were perfusion fixed using 4% paraformaldehyde (PFA, Thermo Fisher, Loughborough, UK) in PBS. After enucleation, the cornea and lens were removed under direct visualisation with an operating microscope in 4% PFA in PBS. After fixation overnight, the eyecups were cryoprotected using a 10-30% sucrose gradient. Eyecups were embedded in optimal cutting temperature (OCT) compound (Tissue-Tek, Sakura Finetek, The Netherlands), frozen on dry ice and stored at -80°C until sectioning. Eyecups were cryosectioned into 16μm sections and affixed to poly-L-lysine coated glass slides (Polysine®; Thermo Scientific, Loughborough, UK). The sections were air-dried and then stored at -20°C until further histological processing.

Human retinal explant culture

Ethical approval was previously obtained to culture samples of retina ex-vivo from patients undergoing retinectomy for complex retinal detachment surgery (REC reference no.10/H0505). Samples used were obtained from three patients with their written consent. A routine 23-gauge (23G) pars plana vitrectomy was done for retinal detachment surgery. Discs of scarred retina were cut with a 23G vitrectomy system (Ocutome; Alcon Surgical,

Irvine, TX), refluxed into the eye, aspirated with a flute needle and placed in balanced salt solution.

Within one hour of removal from the eye, retinectomy samples were transferred using a 5 ml pipette into organotypic culture inserts (BD Falcon, Bedford, MA) and placed in a 24 well plate. 700 μL culture media was added per well consisting of Neurobasal A, L-glutamine (0.08 mM), penicillin (100 U/mL), streptomycin (100 U/mL), B27 supplement (2%), and N2 supplement (1%), all obtained from Invitrogen, UK. Explants were maintained at 34°C in a humidified, 5% CO2 environment.

After 24 hours, media was changed and 10μl of one of rAAV2/2, rAAV2/2 Y444F or rAAV2/8 Y733F (titre 1×10^{12} vg/mL) was added to each well, with 2 wells tested per virus. Media was changed every 48 hours and explants were imaged daily on an inverted epifluorescence microscope (DMIL; Leica, Germany).

14 days post-transfection, explants were fixed overnight in 4% PFA, cryoprotected in 20% sucrose for 1 hour, embedded in OCT compound and frozen on dry ice. Each explant was cut into 16μm sections using a cryostat as above.

Histology and immunohistochemistry

After hydration and 3 × 5 min washes in 0.01M PBS, retinal sections were blocked for 1 hour at room temperature in PBS + 0.1% Triton X-100 + 10% donkey serum. After 3 × 5 min washes, the sections were incubated at 4°C overnight with the primary antibody (PKCalpha 1:1000, Epitomics (1510-1); Calbindin 1:1000 Abcam (ab11426); Brn-3a 1:250, Santa Cruz (sc-31984)) and subsequently for 2 hours at room temperature with secondary antibody (Alexa Fluor 555 donkey anti-rabbit IgG) both in PBS + 0.1% Triton X-100 + 1% serum. After each step, sections were rinsed for 2 × 5 min in PBS + 0.05% Tween20, followed by 1 × 5 min in PBS alone. All sections were counter-stained with Hoechst 33342 (Invitrogen) 1:5000 and mounted with an antifade reagent (Prolong Gold; Invitrogen).

Confocal microscopy

Retinal sections were viewed on a confocal microscope (LSM710; Zeiss, Jena, Germany). GFP-positive cells were located using epifluorescence illumination before taking a series of overlapping XY optical sections, of approximately 0.5μm thickness. Representative images were taken within the region of vector delivery, avoiding the injection site. The fluorescence of Hoechst, GFP and Alexa-555 or 568 were sequentially excited using 350 nm UV laser, 488 nm argon laser and the 543 nm HeNe laser, as appropriate. A stack was built to give an XY projection image as appropriate. Image processing was performed using Volocity (Perkin Elmer, Cambridge, UK) and Image J (Version 1.43, National Institute of Health, http://rsb.info.nih.gov/ij).

In vitro testing of AAV

SH-SY5Y cells (obtained from the American tissue culture collection) were cultured in complete RPMI-1640 media containing L-glutamine (2nM), penicillin (100units/mL),

streptomycin (100mg/mL) all from Sigma-Aldrich UK, and 10% fetal calf serum (GIBCO, Invitrogen, UK). Cells were maintained at 37^{o}C in a 5% CO2 environment.

SH-SY5Y cells were seeded in 96-well culture dishes at a density of 5×10^4 cells/well. After 24 hours, media was changed and proteasome inhibitors (170nM Doxorubicin & 40nM MG-132, Calbiochem, USA) and virus were added. 1μL of virus (1.0×10^{12} vg/mL) was added per well, giving an overall multiplicity of infection (MOI) of approximately 2×10^4 vg/cell. 2 wells were tested per virus, with 3 biological replicates of the experiment performed (total n=6 per group). Media was changed every 48 hours and proteasome inhibitors were maintained in the media throughout. Cells were imaged daily to detect GFP expression using a light microscope (see below). 5 days after transfection, cells were fixed using 4% paraformaldehyde in PBS.

Light microscopy

For the purpose of quantitative analysis of GFP expression, images were taken using the Leica DM IL inverted epifluorescence microscope. Images were obtained at x20 magnification using identical acquisition settings including exposure time, and were saved at a resolution of 1200×1600 pixels.

Image analysis

Image analysis was performed on 8-bit images using ImageJ. Mean pixel grey levels on cSLO images were measured within a circle of 300 pixel diameter. This area was placed within the region of vector delivery, avoiding the needle entry site where associated retinal damage often led to localized increased transduction.

Grey levels on histological fluorescence images were analyzed separately for the RPE, the photoreceptor layer, and the inner retina (including the outer plexiform layer and the inner nuclear layer). This allowed a quantitative analysis of GFP expression within individual retinal layers and thus to assess vector tropism. Regions of defined sizes (RPE: 20×200 pixels, outer nuclear layer: 50×250 pixels, inner retina: 100×250 pixels) were analyzed within areas of highest GFP expression, and the mean pixel grey level was calculated from a plot profile.

Fluorescence images of fixed cells were analysed by calculating mean grey value for each image using ImageJ software, and background levels of fluorescence were subtracted by determining mean grey level of images of untransfected cells.

Statistical analysis

Mean grey levels on cSLO and histological fluorescence images were compared using a two-way analysis of variance test (ANOVA) with mouse strain and rAAV vector type as factors. The Bonferroni post hoc test was applied in all instances to correct for multiple testing, and the significance level was set at 0.05. Mean +/- SEM values are shown in all figures. All statistical analysis was done using Prism 6 for Mac OS X (San Diego, CA, USA).

Supplementary Material

Refer to Web version on PubMed Central for supplementary material.

Acknowledgments

Funding – Wellcome Trust, NIHR Biomedical Research Centres of Oxford and Moorfields, MRC, Fight for Sight, Royal College of Surgeons

References

1. Bainbridge JW, Smith AJ, Barker SS, Robbie S, Henderson R, Balaggan K, et al. Effect of gene therapy on visual function in Leber's congenital amaurosis. N Engl J Med. 2008; 358(21):2231–9. [PubMed: 18441371]
2. Maguire AM, Simonelli F, Pierce EA, Pugh EN Jr, Mingozzi F, Bennicelli J, et al. Safety and efficacy of gene transfer for Leber's congenital amaurosis. N Engl J Med. 2008; 358(21):2240–8. [PubMed: 18441370]
3. Cideciyan AV, Hauswirth WW, Aleman TS, Kaushal S, Schwartz SB, Boye SL, et al. Vision 1 year after gene therapy for Leber's congenital amaurosis. N Engl J Med. 2009; 361(7):725–7.
4. Maclaren RE, Groppe M, Barnard AR, Cottriall CL, Tolmachova T, Seymour L, et al. Retinal gene therapy in patients with choroideremia: initial findings from a phase 1/2 clinical trial. Lancet. 2014
5. Bennett J, Ashtari M, Wellman J, Marshall KA, Cyckowski LL, Chung DC, et al. AAV2 gene therapy readministration in three adults with congenital blindness. Sci Transl Med. 2012; 4(120): 120ra15.
6. Jacobson SG, Cideciyan AV, Ratnakaram R, Heon E, Schwartz SB, Roman AJ, et al. Gene therapy for leber congenital amaurosis caused by RPE65 mutations: safety and efficacy in 15 children and adults followed up to 3 years. Arch Ophthalmol. 2012; 130(1):9–24. [PubMed: 21911650]
7. Testa F, Maguire AM, Rossi S, Pierce EA, Melillo P, Marshall K, et al. Three-year follow-up after unilateral subretinal delivery of adeno-associated virus in patients with Leber congenital Amaurosis type 2. Ophthalmology. 2013; 120(6):1283–91. [PubMed: 23474247]
8. Petrs-Silva H, Dinculescu A, Li Q, Deng WT, Pang JJ, Min SH, et al. Novel properties of tyrosine-mutant AAV2 vectors in the mouse retina. Mol Ther. 2011; 19(2):293–301. [PubMed: 21045809]
9. Dalkara D, Byrne LC, Klimczak RR, Visel M, Yin L, Merigan WH, et al. In vivo-directed evolution of a new adeno-associated virus for therapeutic outer retinal gene delivery from the vitreous. Sci Transl Med. 2013; 5(189):189ra76.
10. Kay CN, Ryals RC, Aslanidi GV, Min SH, Ruan Q, Sun J, et al. Targeting photoreceptors via intravitreal delivery using novel, capsid-mutated AAV vectors. PLoS One. 2013; 8(4):e62097. [PubMed: 23637972]
11. Rabinowitz JE, Rolling F, Li C, Conrath H, Xiao W, Xiao X, et al. Cross-packaging of a single adeno-associated virus (AAV) type 2 vector genome into multiple AAV serotypes enables transduction with broad specificity. J Virol. 2002; 76(2):791–801. [PubMed: 11752169]
12. Vandenberghe LH, Bell P, Maguire AM, Cearley CN, Xiao R, Calcedo R, et al. Dosage thresholds for AAV2 and AAV8 photoreceptor gene therapy in monkey. Sci Transl Med. 2011; 3(88):88ra54.
13. Zhong L, Li B, Mah CS, Govindasamy L, Agbandje-McKenna M, Cooper M, et al. Next generation of adeno-associated virus 2 vectors: point mutations in tyrosines lead to high-efficiency transduction at lower doses. Proc Natl Acad Sci U S A. 2008; 105(22):7827–32. [PubMed: 18511559]
14. Petrs-Silva H, Dinculescu A, Li Q, Min SH, Chiodo V, Pang JJ, et al. High-efficiency transduction of the mouse retina by tyrosine-mutant AAV serotype vectors. Mol Ther. 2009; 17(3):463–71. [PubMed: 19066593]
15. Lochrie MA, Tatsuno GP, Christie B, McDonnell JW, Zhou S, Surosky R, et al. Mutations on the external surfaces of adeno-associated virus type 2 capsids that affect transduction and neutralization. J Virol. 2006; 80(2):821–34. [PubMed: 16378984]

16. Doroudchi MM, Greenberg KP, Liu J, Silka KA, Boyden ES, Lockridge JA, et al. Virally delivered channelrhodopsin-2 safely and effectively restores visual function in multiple mouse models of blindness. Mol Ther. 2011; 19(7):1220–9. [PubMed: 21505421]

17. Ku CA, Chiodo VA, Boye SL, Goldberg AF, Li T, Hauswirth WW, et al. Gene therapy using self-complementary Y733F capsid mutant AAV2/8 restores vision in a model of early onset Leber congenital amaurosis. Hum Mol Genet. 2011; 20(23):4569–81. [PubMed: 21880665]

18. McCarty DM, Fu H, Monahan PE, Toulson CE, Naik P, Samulski RJ. Adeno-associated virus terminal repeat (TR) mutant generates self-complementary vectors to overcome the rate-limiting step to transduction in vivo. Gene Ther. 2003; 10(26):2112–8. [PubMed: 14625565]

19. Yokoi K, Kachi S, Zhang HS, Gregory PD, Spratt SK, Samulski RJ, et al. Ocular gene transfer with self-complementary AAV vectors. Invest Ophthalmol Vis Sci. 2007; 48(7):3324–8. [PubMed: 17591905]

20. Lipinski DM, Thake M, MacLaren RE. Clinical applications of retinal gene therapy. Prog Retin Eye Res. 2013; 32:22–47. [PubMed: 22995954]

21. Allocca M, Doria M, Petrillo M, Colella P, Garcia-Hoyos M, Gibbs D, et al. Serotype-dependent packaging of large genes in adeno-associated viral vectors results in effective gene delivery in mice. J Clin Invest. 2008; 118(5):1955–64. [PubMed: 18414684]

22. Hirsch ML, Agbandje-McKenna M, Samulski RJ. Little vector, big gene transduction: fragmented genome reassembly of adeno-associated virus. Mol Ther. 2010; 18(1):6–8. [PubMed: 20048740]

23. Lopes VS, Boye SE, Louie CM, Boye S, Dyka F, Chiodo V, et al. Retinal gene therapy with a large MYO7A cDNA using adeno-associated virus. Gene Ther. 2013; 20(8):824–33. [PubMed: 23344065]

24. Charbel Issa P, De Silva SR, Lipinski DM, Singh MS, Mouravlev A, You Q, et al. Assessment of tropism and effectiveness of new primate-derived hybrid recombinant AAV serotypes in the mouse and primate retina. PLoS One. 2013; 8(4):e60361. [PubMed: 23593201]

25. Bowes C, Li T, Danciger M, Baxter LC, Applebury ML, Farber DB. Retinal degeneration in the rd mouse is caused by a defect in the beta subunit of rod cGMP-phosphodiesterase. Nature. 1990; 347(6294):677–80. [PubMed: 1977087]

26. Lagali PS, Balya D, Awatramani GB, Munch TA, Kim DS, Busskamp V, et al. Light-activated channels targeted to ON bipolar cells restore visual function in retinal degeneration. Nat Neurosci. 2008; 11(6):667–75. [PubMed: 18432197]

27. Cronin T, Vandenberghe LH, Hantz P, Juttner J, Reimann A, Kacso AE, et al. Efficient transduction and optogenetic stimulation of retinal bipolar cells by a synthetic adeno-associated virus capsid and promoter. EMBO molecular medicine. 2014; 6(9):1175–90. [PubMed: 25092770]

28. Mace E, Caplette R, Marre O, Sengupta A, Chaffiol A, Barbe P, et al. Targeting Channelrhodopsin-2 to ON-bipolar Cells With Vitreally Administered AAV Restores ON and OFF Visual Responses in Blind Mice. Mol Ther. 2014

29. Yin L, Greenberg K, Hunter JJ, Dalkara D, Kolstad KD, Masella BD, et al. Intravitreal injection of AAV2 transduces macaque inner retina. Invest Ophthalmol Vis Sci. 2011; 52(5):2775–83. [PubMed: 21310920]

30. Johnson TV, Martin KR. Development and characterization of an adult retinal explant organotypic tissue culture system as an in vitro intraocular stem cell transplantation model. Invest Ophthalmol Vis Sci. 2008; 49(8):3503–12. [PubMed: 18408186]

31. Lipinski DM, Singh MS, MacLaren RE. Assessment of cone survival in response to CNTF, GDNF, and VEGF165b in a novel ex vivo model of end-stage retinitis pigmentosa. Invest Ophthalmol Vis Sci. 2011; 52(10):7340–6. [PubMed: 21873685]

32. Tolmachova T, Tolmachov OE, Barnard AR, de Silva SR, Lipinski DM, Walker NJ, et al. Functional expression of Rab escort protein 1 following AAV2-mediated gene delivery in the retina of choroideremia mice and human cells ex vivo. Journal of molecular medicine. 2013; 91(7): 825–37. [PubMed: 23756766]

33. Charbel Issa P, Barnard AR, Singh MS, Carter E, Jiang Z, Radu RA, et al. Fundus autofluorescence in the Abca4(-/-) mouse model of Stargardt disease--correlation with accumulation of A2E, retinal function, and histology. Invest Ophthalmol Vis Sci. 2013; 54(8):5602–12. [PubMed: 23761084]

34. Bowles DE, Rabinowitz JE, Samulski RJ. Marker rescue of adeno-associated virus (AAV) capsid mutants: a novel approach for chimeric AAV production. J Virol. 2003; 77(1):423–32. [PubMed: 12477847]

35. Fradot M, Busskamp V, Forster V, Cronin T, Leveillard T, Bennett J, et al. Gene therapy in ophthalmology: validation on cultured retinal cells and explants from postmortem human eyes. Hum Gene Ther. 2011; 22(5):587–93. [PubMed: 21142470]

36. Weng J, Mata NL, Azarian SM, Tzekov RT, Birch DG, Travis GH. Insights into the function of Rim protein in photoreceptors and etiology of Stargardt's disease from the phenotype in abcr knockout mice. Cell. 1999; 98(1):13–23. [PubMed: 10412977]

37. Charbel Issa P, Singh MS, Lipinski DM, Chong NV, Barnard AR, Maclaren RE. Optimization of in vivo confocal autofluorescence imaging of the ocular fundus in mice and its application to models of human retinal degeneration. InvestOphthalmol VisSci. 2012

Europe PMC Funders Author Manuscripts

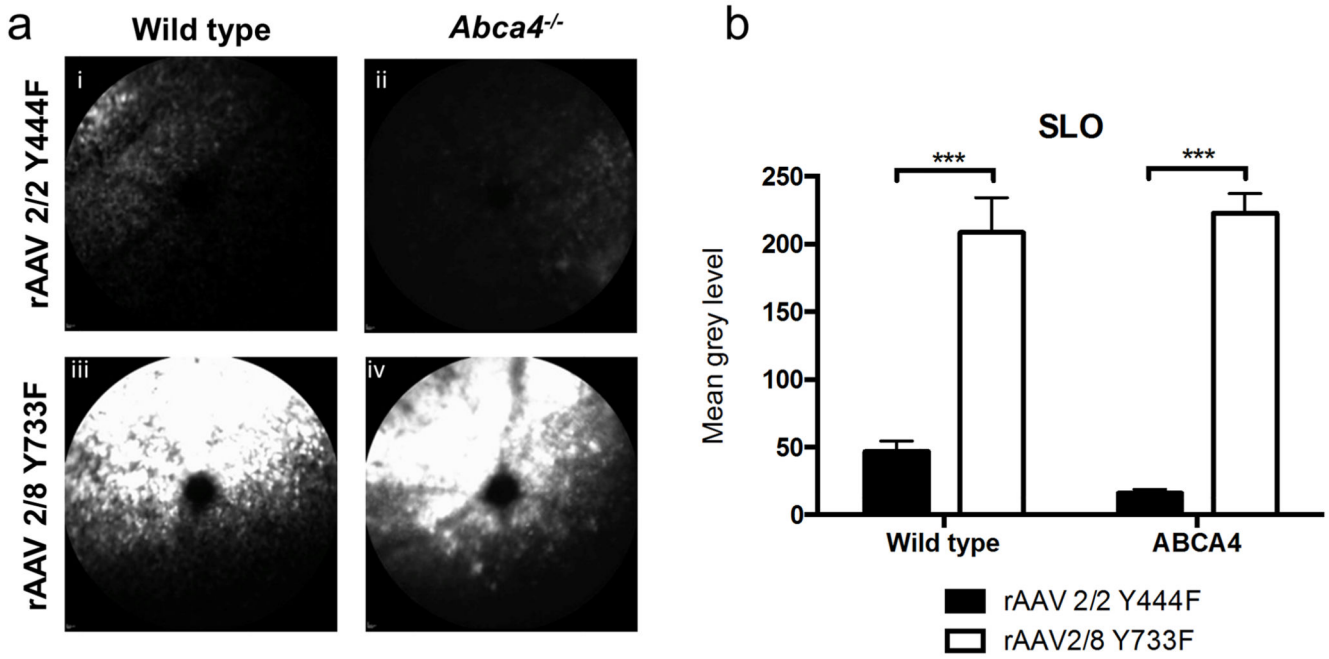

Figure 1.

Analysis of *in vivo* measurement of fluorescence intensity 3 weeks after subretinal injection of single stranded rAAV2/2 (Y444F) and rAAV2/8 (Y733F). Figure 1a, i-iv: Representative *in vivo* confocal scanning laser ophthalmoscopy (cSLO) 488 nm-fluorescence images in wild type and *Abca4*$^{-/-}$ mice. The subretinal injection was placed in the superior fundus, except for image ii where the injection area is on the right hand side. Figure 1b: Quantification of fluorescence derived from expression of green fluorescent protein (GFP) used as reporter protein is shown in the bar graph (mean±SEM). 5-6 eyes were analyzed per group.

Europe PMC Funders Author Manuscripts

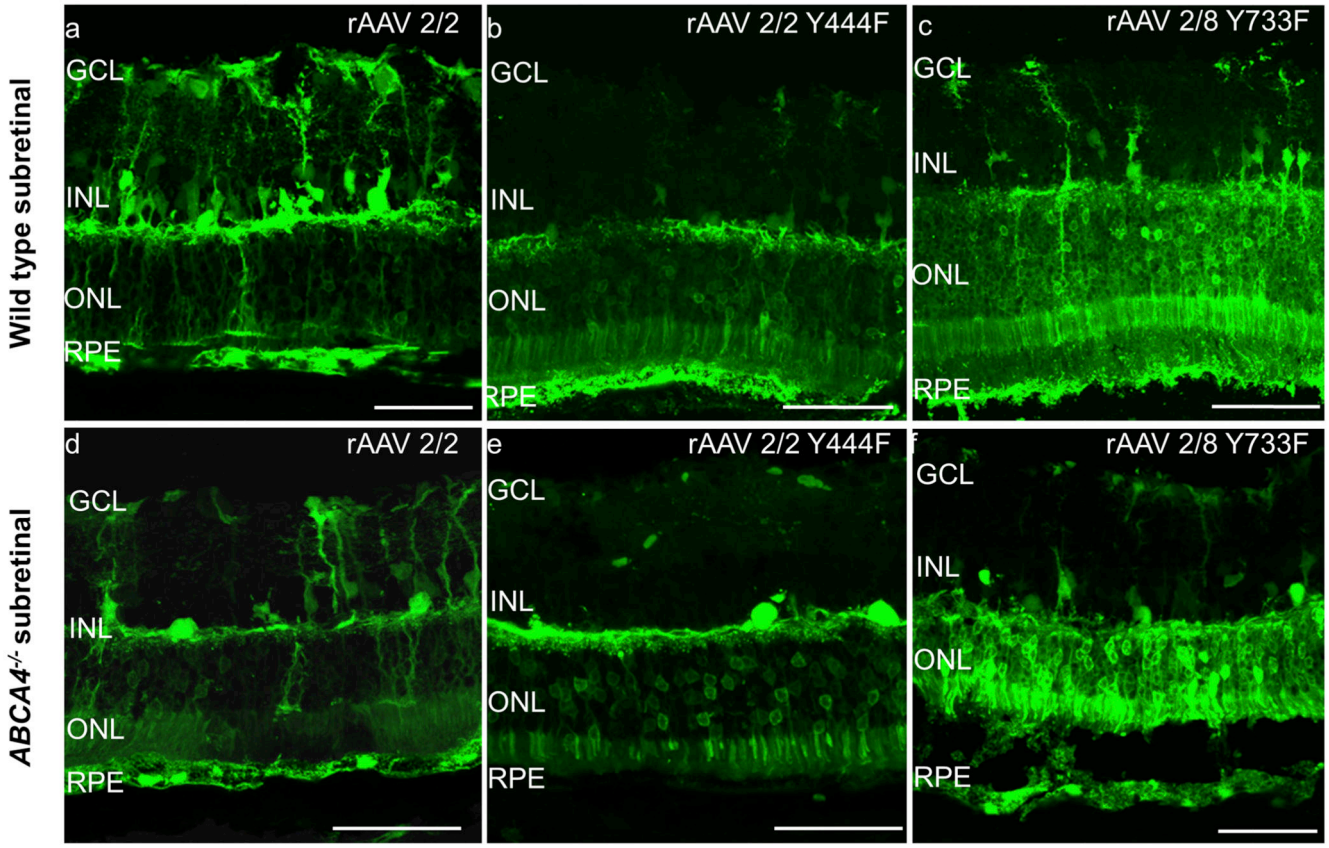

Figure 2.

GFP fluorescence patterns of different rAAV serotypes following subretinal injection in wild type (WT) C57BL/6 and *Abca4*$^{-/-}$ mice. Images a-f are confocal stacks illustrating overall GFP expression patterns (green). GCL= ganglion cell layer, INL= inner nuclear layer, ONL= outer nuclear layer, RPE= retinal pigment epithelium. Scale bar 50 μm.

Europe PMC Funders Author Manuscripts

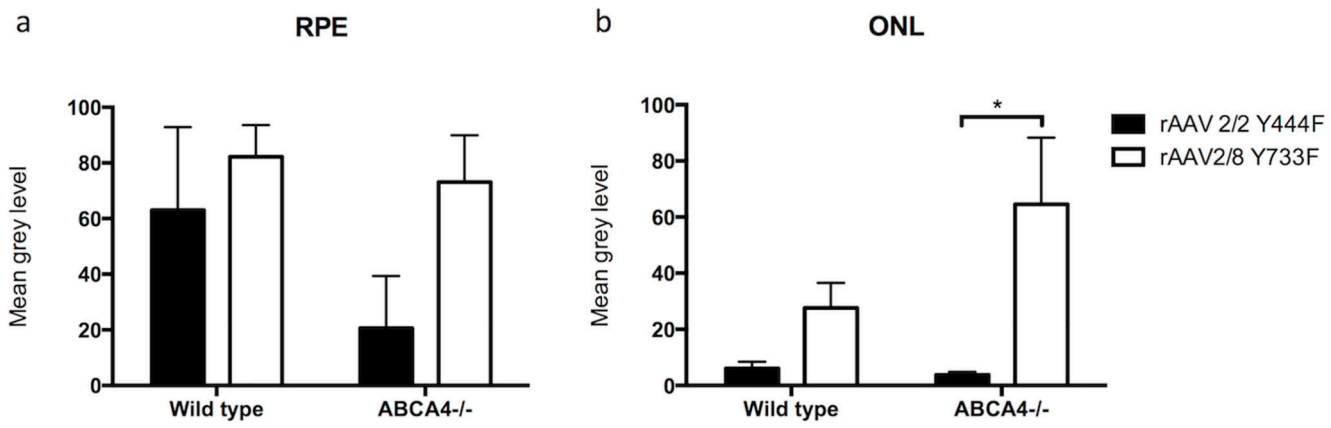

Figure 3.

Quantitative analysis of green fluorescent protein (GFP) fluorescence intensity on histological sections in eyes that underwent subretinal injection of rAAV2/2 Y444F and rAAV2/8 Y733F capsid mutant AAV serotypes expressing GFP (mean±SEM). The grey level analysis represents an estimate for the level of transgene expression within individual cell layers. 4 to 6 eyes were analysed per group.

Europe PMC Funders Author Manuscripts

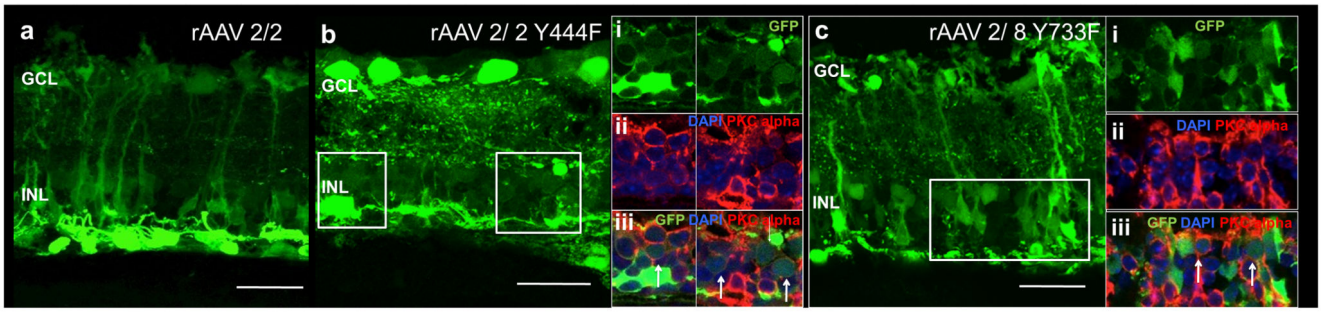

Figure 4.

GFP fluorescence patterns of different rAAV serotypes following subretinal injection in *Pde6b*$^{rd1/rd1}$ mice. The main images a-c are confocal stacks illustrating overall GFP expression patterns (green). The boxed regions are enlarged and shown as confocal slices in panels bi-iii and ci-iii. Images show GFP expression (green), nuclear labeling (blue) and immunostaining with with anti-PKCalpha antibody, identifying bipolar cells (red). Co-localisation of red and green signals therefore indicates instances of viral transduction of bipolar cells. GCL= ganglion cell layer, INL= inner nuclear layer. Scale bar 30μm.

Europe PMC Funders Author Manuscripts

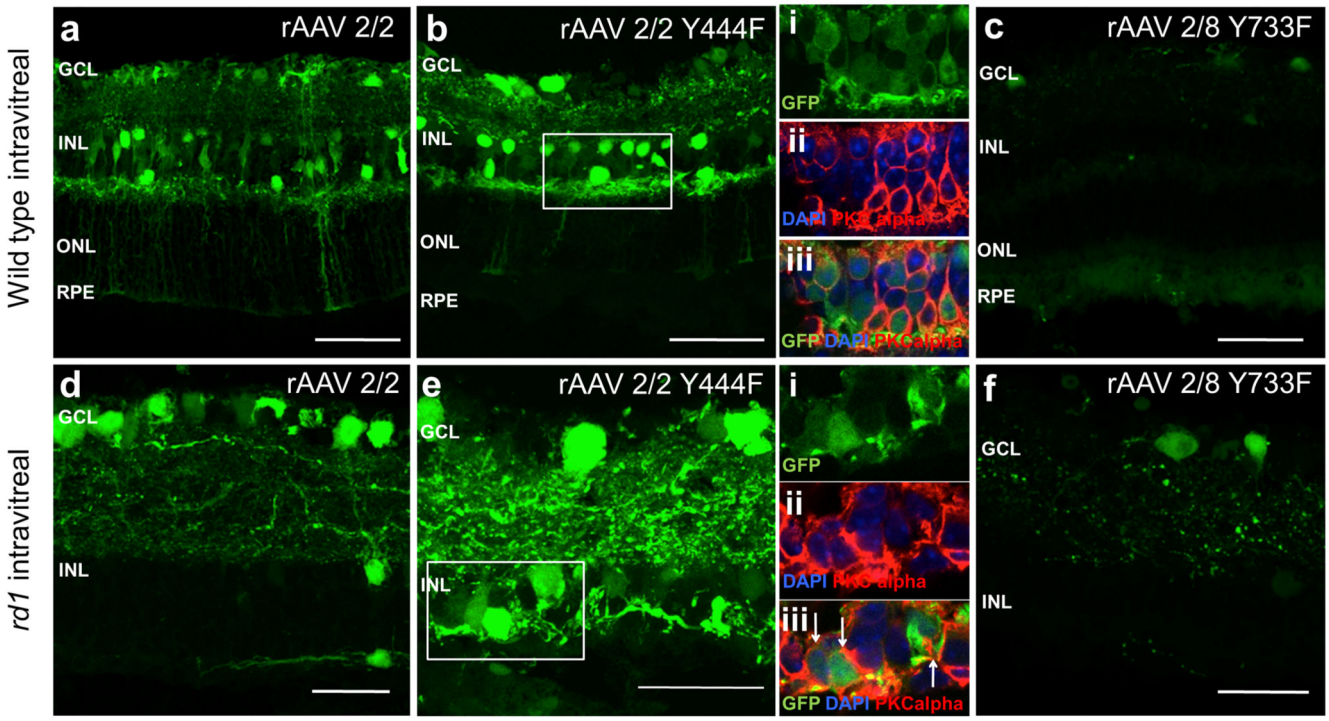

Figure 5.

GFP fluorescence patterns of different rAAV serotypes following intravitreal injection in wild type (WT) C57BL/6 and *Pde6b*$^{rd1/rd1}$ (rd1) mice. The main images a-f are confocal stacks illustrating overall GFP expression patterns (green). The boxed regions are enlarged and shown as confocal slices in panels bi-iii and ei-iii. Images show GFP expression (green), nuclear labeling (blue) and immunostaining with anti-PKCalpha antibody identifying bipolar cells (red). Colocalisation of red and green signals therefore indicates instances of viral transduction of bipolar cells. GCL= ganglion cell layer, INL= inner nuclear layer, ONL=outer nuclear layer, RPE= retinal pigment epithelium. Scale bar 50 μm for images a-c, 30μm for images d-f.

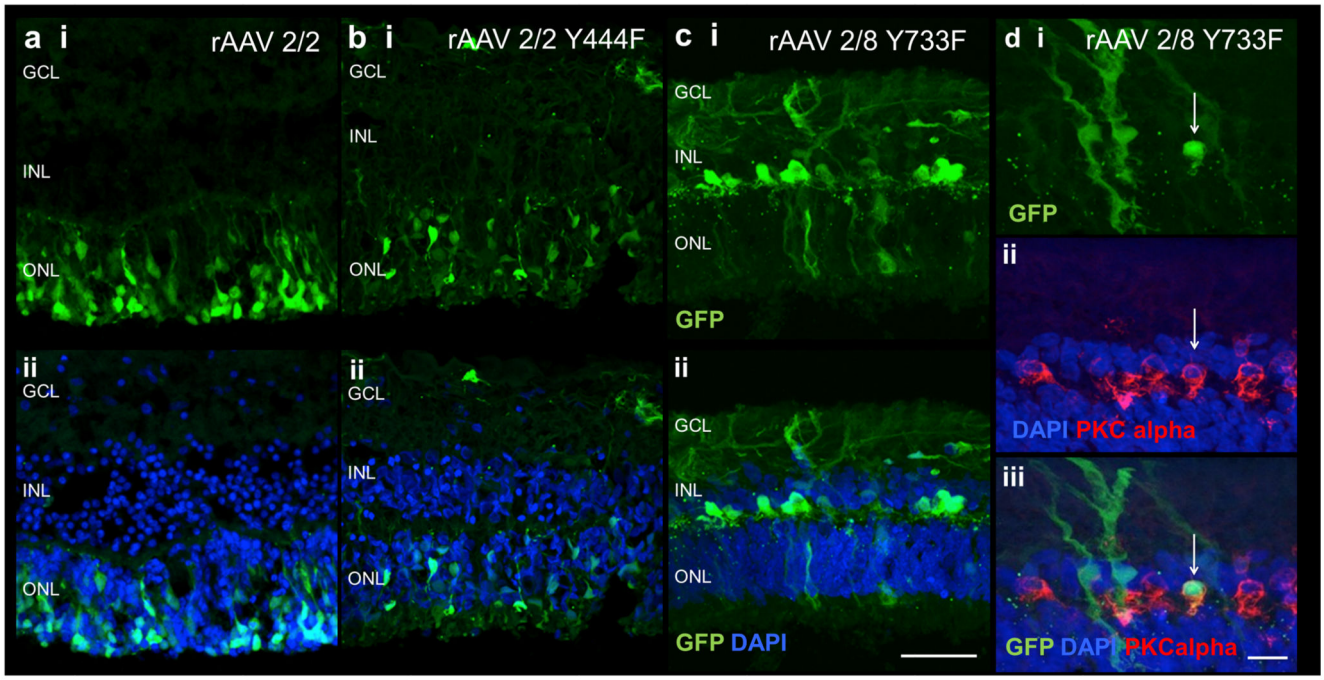

Figure 6.

GFP fluorescence following *ex vivo* administration of AAV vectors in human retinal tissue. GFP expression in explants following rAAV 2/2 (a), rAAV2/2 Y44F (b) and rAAV2/8 Y733F (c) exposure. Histological cross-sections of specimens show expression of GFP (green, panel i) and merge with DAPI (blue, panel ii) for each vector. Images d shows colocalisation of GFP (green) in bipolar cells identified by PKC alpha immunostaining (red) demonstrating human bipolar cell transduction. GCL= ganglion cell layer; INL= inner nuclear layer, ONL= outer nuclear layer. Scale bar 50μm for images a-c, 10μm for images d.

Europe PMC Funders Author Manuscripts